IOP Conf. Series: Materials Science and Engineering **1344** (2026) 012033 doi:10.1088/1757-899X/1344/1/012033

Compact nitrogen pulsating heat pipes – Experimental thermal analysis with numerical insights

Marcin Opalski[1,2], Tisha Dixit[1], Gilles Authelet[1], Vadim Stepanov[1], Théophile Benoit[1], Sławomir Pietrowicz[2], and Bertrand Baudouy[1]

[1]Université Paris-Saclay, CEA, IRFU, Département des Accélérateurs, de la Cryogénie et du Magnétisme, 91191 Gif-sur-Yvette, France
[2] Wrocław University of Science and Technology, Faculty of Mechanical and Power Engineering, Department of Thermodynamics and Renewable Energy Sources, Wybrzeże Wyspiańskiego 27 St., 50-370 Wrocław, Poland

E-mail: marcin.opalski@pwr.edu.pl

Abstract.

With the growing adoption of cryocoolers, there is a demand for efficient thermal links to the cold stages. This demand can be addressed by pulsating heat pipes (PHPs) offering a promising solution at cryogenic temperatures. Despite progress, current literature does not allow precise prediction of PHP performance at cryogenic conditions. To address this gap, we propose a numerical model developed in OpenFOAM. The implementation of the model includes customized conservation equations, thereby incorporating phase change dynamics based on the Volume of Fluid approach. In order to validate this numerical model, a compact PHP has been constructed. A setup has been built to test the designed PHP at different cryogenic temperature ranges. The cooling is provided by a two-stage cryocooler having a cooling capacity of about 28 W at 77 K. The PHP is fabricated from stainless steel tubes with an inner diameter of 1.3 mm. It has projected overall dimensions of approximately 0.19 m x 0.11 m. Nitrogen is used as the working fluid with operating temperatures ranging from 77.3 to 94 K. We also present preliminary results validated against experimental data demonstrating the precision of the implemented model in predicting the thermal performance of cryogenic PHPs.

1 Introduction

Pulsating heat pipe provide an effective solution for heat extraction and thermal transport, particularly under ambient conditions [1]. Their application in cryogenics remains at an early stage. The increasing shift from liquid cryogens to cryocooler-based systems has triggered a growing interest in such compact and efficient thermal transfer devices [2]. Cryocoolers require thermal links that are typically made of copper or aluminum with a high residual resistivity ratio, available in rigid or flexible configurations depending on system integration constraints. Although these thermal links are widely used, they suffer from limitations such as high density, higher material cost, and thermal conductivities that may not guarantee effective heat transfer to the cold source.

At CEA Paris-Saclay, several experimental studies have investigated the use of cryogenic PHPs as thermal links for cryocoolers examining orientation effects, geometrical parameters, filling ratio and startup behavior [3, 4, 5, 6, 7]. These works have demonstrated that PHPs can outperform oxygen-free, high-conductivity copper in equivalent thermal conductivity while remaining lightweight and passive in operation. A central objective of these studies is the integration of PHPs into the thermal architecture of superconducting magnet systems, where conventional cryogen-based cooling has limitations, especially at very high magnetic fields. Similar objectives are being pursued by other research groups working on the integration of cryogenic PHPs for magnet cooling as thermal links under conduction cooling with cryocooler [8, 9, 10]. Their complex and partially unpredictable operation, often described using empirical criteria such as the critical Bond number [11, 12], remains a barrier to design and control. For example, Dixit et al. [7] demonstrated that Bond-number-based predictions do not always align with the observed PHP performance in cryogenic regimes. Furthermore, cryofluids for phase-change operation near atmospheric pressure tend to exhibit narrow temperature ranges, further complicating the system design.

Several recent numerical studies have addressed cryogenic PHP behavior using CFD tools such as ANSYS Fluent [13, 14, 15, 16]. Although they provide useful insights into system dynamics at low temperatures, the closed-source nature of Fluent constrains access to the numerical formulation, limits user control over solver internals and often requires external user defined functions to modify physics. This restricts the reproducibility and adaptation of models to more complex experimental geometries, especially when customized boundary conditions or conservation constraints are needed. These limitations motivate the development of alternative approaches based on open-source platforms. The present work extends previous studies on ambient temperature and PHP modeling [17, 18] to the cryogenic regime. Our earlier simulations were based on simpler geometry and employed a liquid cryogen to cool the condenser section instead of a cryocooler [19].

Herein, we introduce an original experimental setup that features compact five-loop PHPs. These configurations offer a simple domain that can be feasibly analyzed using computational fluid dynamics without requiring extensive computational resources. Comparable loop counts have previously been investigated in experimental studies under cryogenic conditions [20, 21], although without focusing on numerical modeling. The present work fills this gap by combining experimental measurements with a validated numerical model, enabling a consistent comparison between simulated and observed thermal behavior.

2 Experimental Setup and Design Process

In the experiment, a Sumitomo CH-208L 10K two-stage cryocooler is used, featuring a nominal cooling capacity of 28 W at 77 K under no-load conditions, according to the manufacturer's specifications [22]. The PHP is constructed from stainless steel capillaries with an internal diameter of 1.3 mm. The evaporator and condenser plates, as well as the radiation shield and the cryocooler coupling block, are machined from oxygen-free copper (CuC1). The copper plates are sized 50 mm × 110 mm, while the total longitudinal length of the assembly is 190 mm. The entire structure is mounted on the first stage of the cryocooler which maintains the condenser temperature. It was controlled at 77.3 K using heaters, with active regulation provided by a Lake Shore CTC100 controller. The temperature was measured in six locations using Cernox® 1050 sensors. Sensors were embedded in the machined grooves of the copper evaporator plate and three in the condenser. Absolute pressure was monitored in the feedthrough pipe outside the cryostat. The heat input to the evaporator was supplied via kapton heaters powered by a Keithley power supply. The placement of the sensor slots and the overall physical layout of PHP is illustrated in Figure 1.

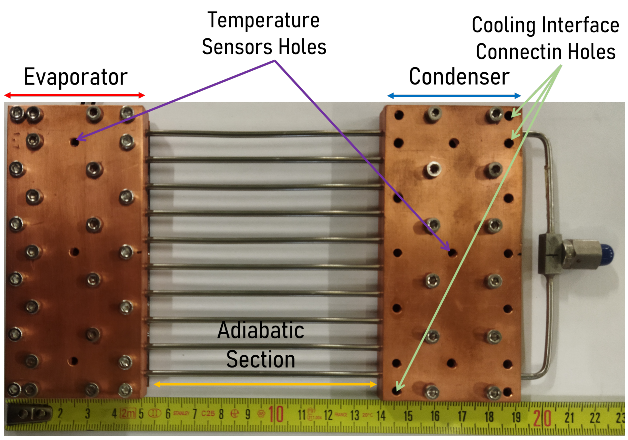

Figure 1. Pictorial view of cryogenic PHP with marked thermal sections and construction details.

The PHP is in vertical position and filled with liquid nitrogen to 50% of its internal volume using an external gas supply system consisting of a buffer vessel, a dry scroll pump, and a turbomolecular pump to establish vacuum. The filling procedure follows a standard procedure described in detail in [23]. The results of the thermal and hydraulic response tests are presented in Figures 2, which show the behavior of the system under applied heat loads ranging from 0 to 25 W. The figure includes the average temperatures recorded by three sensors placed on the surfaces of the evaporator and condenser, as well as the absolute pressure measured in the system.

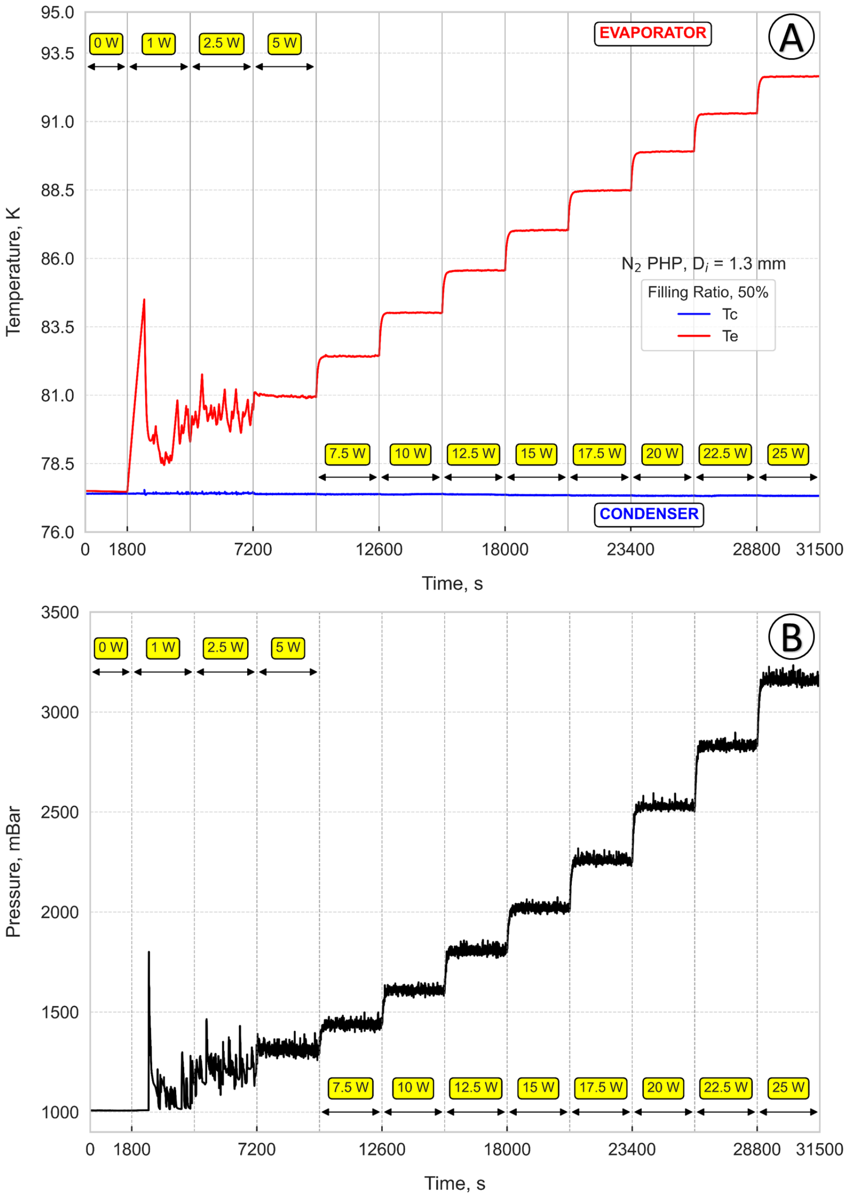

Figure 2. Thermal (A) and hydraulic (B) response of the PHP for a 50% filling ratio under heat loads from 0 to 25 W. The curves show the time evolution of averaged evaporator and condenser temperatures, along with the absolute pressure measured in the system.

The initial temperature and pressure fluctuations observed in Figure 2 are attributed to insufficient heat input in the low-power regime, which was not high enough to sustain stable PHP operation. The PHP demonstrates stable performance between 5 W and 25 W with the evaporator temperature increasing with an increase in the applied heat load. The absolute pressure exhibited exponential growth in this range. The 25 W limit represents the actual upper bound of the cryocooler's cooling capacity.

3 Numerical Insights

The numerical 2–D model to predict the thermohydraulic performance of cryogenic PHP is based on the approach previously developed by Opalski et al. [19]. The simulations were performed using the OpenFOAM framework and rely on the VOF method to resolve the two-phase flow behavior within the pulsating heat pipe. A two-dimensional computational domain was used, representing the geometry of the present five-loop PHP. Although the geometry differs from that in [19], the mesh resolution across the internal tube diameter was kept identical to that study to ensure comparable accuracy with 10 elements in fluid and 3 elements in the radial direction. The experimental vertical orientation was reproduced in the simulations by setting the gravity vector. Turbulence was modeled using the standard k–ε model with standard wall functions (`kqRWallFunction`, `epsilonWallFunction`, `nutkWallFunction`) applied on all fluid-solid interfaces. The general structure of the solver algorithm is presented in Figure 3, which combines both the control logic of the simulation loop and the iterative sequence executed within the PIMPLE algorithm. The structure of the algorithm includes an update of the thermophysical properties, resolution of the phase change model through the interfacial mass transfer terms, and solution of the coupled equations for the phase fraction, momentum, energy, and pressure. Turbulence is corrected after each iteration cycle, and time advancement is based on adjustable time-stepping with field write-out at selected intervals. In addition to the numerical scheme, Figure 3 also displays the evolution of the interface in the early stages resolved by the VOF method. Four selected time frames between 0 and 2 s illustrate the rapid formation of vapor-liquid structures from a randomized initial distribution. Although this initialization is not physically accurate, it was adopted because of the lack of experimental information on the actual phase arrangement at the start of the test and was previously successfully applied in [18, 19]. Given the total simulated physical time of 350 s, this assumption allows surface tension effects to dominate and naturally form interfacial patterns without artificial enforcement.

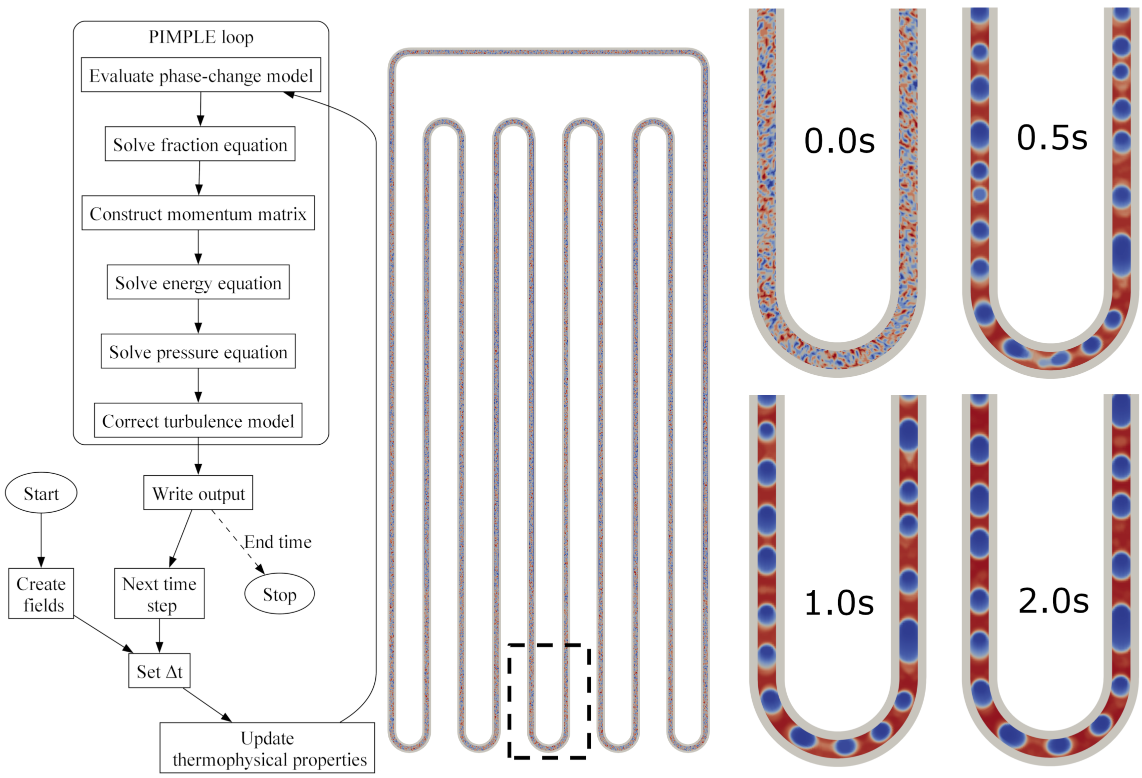

Figure 3. Numerical algorithm and early interface evolution in the PHP domain. Left: simulation loop structure with VOF-PIMPLE sequence, Right: vapor–liquid phase distribution from randomized initial field over 0–2 s in case of 50% fill ratio, 15 W heat load in marked region.

Three heating power loads were considered: 10, 15, and 20 W. For each case, the simulated temperature of the evaporator wall and the domain-averaged pressure were evaluated throughout the simulation time and compared with experimental measurements. The total simulation time was set to 350 s to

IOP Conf. Series: Materials Science and Engineering **1344** (2026) 012033 doi:10.1088/1757-899X/1344/1/012033

ensure that the final 100 s reached a statistically steady regime, during which pressure and temperature fluctuations remained within a narrow range. Figure 4 presents the time evolution of both quantities for each input power level. The experimental reference values, averaged over the final 15 minutes of steady-state operation, are indicated as horizontal lines in the plots to facilitate direct comparison. The average pressure of the domain was calculated by integrating the values in both the liquid and vapor regions numerically, while the wall temperatures were sampled directly at the liquid–solid interface on the evaporator surface. In the simulations, the initial temperature was set equal to the condenser temperature ($T_0 = T_c = 77.3$ K) and held constant on the condenser patch throughout the run, while heating was applied at the evaporator through a prescribed uniform heat flux corresponding to the selected power input. The initial pressure was uniform at 1000 mbar.

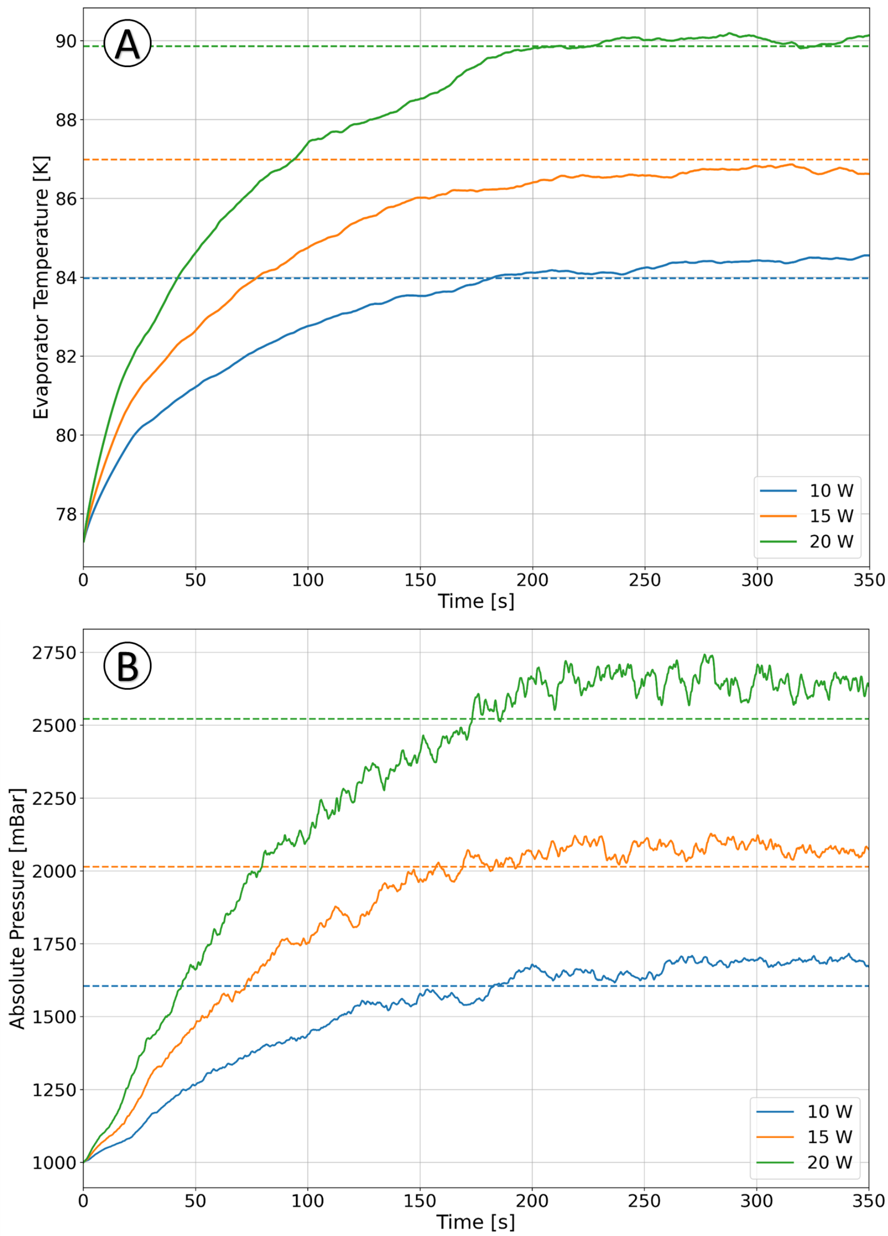

Figure 4. Time evolution of evaporator wall temperature (A) and domain-averaged pressure (B) obtained from numerical simulations for a 50% fill ratio and heating powers of 10, 15, and 20 W. Horizontal lines indicate experimental values averaged over the final 15 minutes of steady-state operation.

In contrast to the surface average temperature from the simulation, the experimental data came from sensors embedded in machined grooves of the copper evaporator and condenser plates. The stainless steel capillary tubes were sandwiched between the plates. Each plate housed three sensors, and the reported values represent their average. Due to the thermal inertia of the copper structure and the indirect thermal path, experimental temperature readings exhibit partial damping, which reduces the amplitude of observed oscillations. The pressure was measured outside the cryostat. The filling line and enclosed volume dampen transient fluctuations, reducing the observed dynamic range of the pressure signal. Unlike the experiment, the numerical model captures local vapor formation and flow instabilities, directly resolving the resulting pressure variations through coupled mass, momentum, and energy transport equations. Although the numerical solver may overestimate instantaneous fluctuations, the experimental setup may underestimate them due to distributed sensing and structural damping. Thus, both methods are subject to limitations, the simulation neglects mechanical damping, thermal contact resistance, and the spatial filtering inherent to sensor design, while the experiment intrinsically smooths transients due to system inertia and sensor placement. Comparison of the experimental and numerical performance is shown in terms of thermal resistance. Thermal resistance R is defined as the ratio of the temperature difference between the evaporator and the condenser to the applied heat load, that is, $R = (T_\mathrm{e} - T_\mathrm{c})/Q$. The comparison of the average thermal resistance values for this cryogenic PHP obtained from the numerical model and from the experiment with the filling ratio 50% is presented in the summary table 1.

Table 1. Comparison of experimental and numerical thermal resistance values and relative error

Case	R_exp (K/W)	R_num (K/W)	Relative error (%)
10 W	0.6675	0.7191	7.73
15 W	0.6457	0.6258	3.08
20 W	0.6280	0.6377	1.55

4 Summary and Future Work

The present work reports experimental and numerical results obtained for a five-loop cryogenic PHP with nitrogen as the working fluid. The experimentally measured thermal resistance values ranged from 0.6 to 0.72 K/W for steady-state heat loads between 10-25 W and the numerical predictions closely matched these values, with relative errors below 8%.

In addition to accurately capturing global thermal parameters, the numerical model successfully reproduced essential thermohydraulic phenomena, including characteristic temperature changes and physically consistent pressure oscillations. These results demonstrate the ability of the model to represent the dominant thermal-fluid mechanisms governing PHP operation under cryogenic conditions. This provides a solid foundation for further investigations into internal flow dynamics and vapor-liquid interactions, which remain experimentally inaccessible.

Future studies will focus on extending the numerical validation to a broader range of operating conditions and refining the characterization of internal flow regimes, including directional statistical analysis to evaluate mean circulation effects. Additional efforts will aim to enhance numerical robustness, particularly under conditions involving intense phase change and steep thermophysical gradients. Parametric analyzes will also be carried out to explore the geometric sensitivity of PHP, with particular emphasis on the influence of capillary diameter on flow patterns and thermal performance.

References

[1] Mameli M, Besagni G, Bansal PK, Markides CN. Innovations in Pulsating Heat Pipes: From Origins to Future Perspectives. Applied Thermal Engineering. 2022;203:117921.
[2] Baudouy B. Heat Transfer and Cooling Techniques at Low Temperature. In: Bailey R, editor. Proceedings of the CERN Accelerator School: Superconductivity for Accelerators. CERN–2014–005. Erice, Italy: CERN; 2014. .
[3] Bruce R, Barba M, Bonelli A, Baudouy B. Thermal performance of a meter-scale horizontal nitrogen Pulsating Heat Pipe. Cryogenics. 2018;93:66-74.
[4] Barba M, Bruce R, Bouchet F, Bonelli A, Baudouy B. Effects of filling ratio of a long cryogenic Pulsating Heat Pipe. Applied Thermal Engineering. 2021;194:117072.

[5] Barba M, Bruce R, Bouchet F, Bonelli A, Baudouy B. Effect of the thermo-physical properties of the working fluid on the performance of a 1-m long cryogenic horizontal pulsating heat pipe. International Journal of Heat and Mass Transfer. 2022;187:122458.
[6] Dixit T, Authelet G, Mailleret C, Gouit F, Stepanov V, Baudouy B. High performance and working stability of an 18W class neon pulsating heat pipe in vertical/horizontal orientation. Cryogenics. 2023;132:103670.
[7] Dixit T, Daval M, Authelet G, Mailleret C, Gouit F, Stepanov V, et al. Oversized diameter helium pulsating heat pipe. Applied Thermal Engineering. 2024;251:123613.
[8] Mito T, Natsume K, Yanagi N, Tamura H, Tamada T, Shikimachi K, et al. Development of highly effective cooling technology for a superconducting magnet using cryogenic OHP. IEEE Transactions on Applied Superconductivity. 2010;20(3):2023 – 2026.
[9] Liang Q, Li Y, Wang Q. Cryogenic Oscillating Heat Pipe for Conduction-Cooled Superconducting Magnets. IEEE Transactions on Applied Superconductivity. 2017 12;PP:1-1.
[10] Fonseca L, Miller F, Pfotenhauer J. A Helium Based Pulsating Heat Pipe For Superconducting Magnets. AIP Conference Proceedings. 2013 12;1573.
[11] Akachi H. Pulsating heat pipes. In: Proc. 5th International Heat Pipe Symp., 1996; 1996. p. 208-17.
[12] Khandekar S, Groll M. On the definition of pulsating heat pipes: An overview. Proc 5th Minsk Int Conf (Heat Pipes, and Refrigerators). 2003 01:116-28.
[13] Yang D, Bu Z, Jiao B, Wang B, Gan Z. Numerical Study of Heat Transfer and Fluid Flow Characteristics of a Hydrogen Pulsating Heat Pipe with Medium Filling Ratio. Energies. 2024 06;17:2697.
[14] Bu Z, Li S, Zhao S, Jiao B, Su R, Wang B, et al. Thermo-hydrodynamic analysis of a nitrogen flat-plate pulsating heat pipe using CFD modeling and visualization experiments. International Communications in Heat and Mass Transfer. 2024;159:108029.
[15] Sagar KR, Naik HB, Mehta HB. Numerical study of liquid nitrogen based pulsating heat pipe for cooling superconductors. International Journal of Refrigeration. 2021;122:33-46.
[16] Singh A, Ghosh I. Numerical Investigations of a Single Loop Pulsating Heat Pipe for Cryogenic Applications. ASME Journal of Heat and Mass Transfer. 2024 10:1-30.
[17] Błasiak P, Opalski M, Parmar P, Czajkowski C, Pietrowicz S. The Thermal—Flow Processes and Flow Pattern in a Pulsating Heat Pipe—Numerical Modelling and Experimental Validation. Energies. 2021;14(18).
[18] Opalski M, Czajkowski C, Błasiak P, Nowak AI, Ishimoto J, Pietrowicz S. Comprehensive numerical modeling analysis and experimental validation of a multi-turn pulsating heat pipe. International Communications in Heat and Mass Transfer. 2024;159:107990.
[19] Opalski M, Dixit T, Baudouy B, Błasiak P, Ishimoto J, Pietrowicz S. Modeling of cryogenic pulsating heat pipe using CFD techniques. Cryogenics. 2025;147:104061.
[20] Natsume K, Mito T, Yanagi N, Tamura H, Tamada T, Shikimachi K, et al. Heat transfer performance of cryogenic oscillating heat pipes for effective cooling of superconducting magnets. Cryogenics. 2011;51(6):309-14. Special Issue: ACASC 2009.
[21] Shi Y, Yan J, Zhou Y, Xu D, Li L. Experimental study on nitrogen pulsating heat pipes with different heat transmission distances and configurations. Cryogenics. 2024;141:103898.
[22] Sumitomo (SHI) Cryogenics of America, Inc . CH-208L 10K Cryocooler Series – Technical Specifications;. Accessed: 2025-06-02. Available from: `https://shicryogenics.com/product/ch-208l-10k-cryocooler-series/`.
[23] Higueras MAB. Study of Meter-scale Horizontal Cryogenic Pulsating Heat Pipes [Ph.D. thesis]. Université Paris-Saclay, Université Paris-Sud; 2019. Available from: `https://theses.hal.science/tel-02370413`.